Complexity-Reduced MUSIC Using Bicubic Interpolation to ISAC in Near-Field Region

Thiago Augusto Bruza Alves, David William Marques Guerra, José Carlos Marinello, Taufik Abrão

***Abstract*— Integrated sensing and communication (ISAC) systems rely on accurate localization algorithms, commonly implemented via computationally demanding methods such as the multiple signal classification (MUSIC) algorithm. Typically, fine-grid searches required by MUSIC lead to high computational complexity, posing practical limitations for real-time implementations. This paper introduces bicubic interpolation applied to coarse-grid MUSIC pseudo-spectra to significantly reduce complexity without sacrificing localization accuracy. The search grid is initially defined over a uniformly spaced Cartesian coordinate system and subsequently transformed into polar coordinates to enable accurate steering vector evaluation within the MUSIC algorithm. This formulation allows for the direct application of interpolation techniques to the resulting pseudo-spectrum. The simulation results demonstrate that the proposed interpolation strategy substantially decreases the computational load while maintaining competitive precision compared to traditional fine-grid MUSIC methods. Performance evaluations in terms of root mean square error (RMSE), computational time and computational complexity analysis (flops) support the effectiveness and potential application of the proposed approach in future ISAC deployments.**

I. Introduction

ISAC, a promising paradigm for future wireless systems beyond 5G, integrates radar-like sensing with data communication using shared spectral and hardware resources [1]. Accurate localization is fundamental in ISAC systems for enabling key functions such as beamforming, resource allocation, and environment mapping. Although the MUSIC 2D algorithm offers high resolution and is widely adopted, its dependence on dense two-dimensional grid searches results in prohibitive computational costs, particularly for the large-scale antenna arrays envisioned for 6G networks [2].

Recent research offers strategies to reduce this complexity while maintaining localization accuracy. [3] proposed a near-field localization approach using an electric field model, deriving closed-form estimators with low-overhead maximum-likelihood refinement. [4] introduced a sparse estimation framework with the sparse iterative covariance-based estimation (SPICE) algorithm in an exact near-field model, showing robustness with limited snapshots. [5] combined focusing and alternating oblique projection to improve coherent source resolution and mitigate coherence errors. [6] also developed hybrid sensing architectures with reconfigurable intelligent surfaces for unified near- and far-field treatment through adaptive grid searches. Furthermore, [7] applied interpolation and denoising on coprime coarrays for gridless, parameter-free high-resolution direction-of-arrival (DOA) estimation.

To further improve computational efficiency, zoom-in MUSIC (reduced-dimension MUSIC) [8] was introduced. This method reformulates the joint estimation problem by projecting the received signal onto a lower-dimensional subspace, enabling a single one-dimensional spectral search. Despite its simplicity, zoom-in MUSIC maintains high-resolution capability and offers a compelling alternative in resource-constrained systems.

Bicubic interpolation [9], [10], widely utilized in image processing, emerges as an attractive solution to refine coarse-grid pseudo-spectra into high-resolution outputs with minimal computational overhead. However, its direct application is hindered because the MUSIC pseudo-spectrum in radar-like ISAC systems is typically computed in polar coordinates, where interpolation becomes non-trivial.

This paper proposes a practical and computationally efficient approach: adopting a Cartesian search grid for coarse MUSIC estimation enables the direct application of bicubic interpolation. Refining the coarse pseudo-spectrum through bicubic methods significantly reduces computational complexity while preserving sub-meter localization accuracy under practical signal-to-noise ratios, making it highly suitable for real-time ISAC scenarios.

The remainder of this paper is organized as follows: Section II describes the system model and the proposed interpolation procedure. Section III presents simulation results and performance evaluations. Finally, conclusions and perspectives are drawn in Section IV.

II. System Model

Consider an ISAC system where a base station (BS) (or an equivalent transmission point) emits a signal primarily intended for communication, for example, a Quadrature Amplitude Modulation (QAM) waveform. This communication signal, upon reflection from a static user/target, is also leveraged for sensing. The system comprises a uniform linear array (ULA) with $M = 2N + 1$ sensor elements separated by $\lambda/4$ wavelength spacing [4], [8], [11], operating at frequency f_c. The sensing objective is to localize a near-field users/targets positioned within a two-dimensional (2D) region. The parameters (r_k, θ_k) denote the direction-of-arrival (DOA) and

This work was supported in part by the CAPES (Financial Code 001) and the National Council for Scientific and Technological Development (CNPq) of Brazil under Grant 310681/2019-7.

T. A. B. Alves and T. Abrão are with the Depar. of Elect. Eng. (DEEL). State Univ. of Londrina (UEL). Londrina, PR, Brazil. Email: thiagobruza@outlook.com; taufik@uel.br. D. W. M. Guerra is with the Depar. of Elet. and Systems (DES). Fed. Univ. of Pernambuco, Brazil. Email: david.guerra@ufpe.br. J.C. Marinello is with Depart. of Elect. Eng. Fed. Tech. Univ. of Paraná. Cornélio Procópio, PR, Brazil. Email: jcmarinello@utfpr.edu.br.

distance of the k-th source related to the center of the array. This localization of the fixed or low mobility target/user is performed by processing L discrete time snapshots of the received signal. The signal captured by the m-th sensor at time instant t, where m ranges from $-N$ to N and $t = 1, \ldots, L$, is expressed as

$$y_m(t) = \sum_{k=1}^{K} s_k(t) e^{j\frac{2\pi}{\lambda}(d_m^{(k)} - d_0^{(k)})} + n_m(t), \tag{1}$$

where the quantity $d_m = \sqrt{(x_k - x_m)^2 + y_k^2}$ represents the distance between the k-th source located at position (x_k, y_k) and the m-th sensor at lateral displacement $x_m = md$, while $d_0 = \sqrt{x_k^2 + y_k^2}$ is the distance from the same source to the reference sensor located at the origin (*i.e.*, for $m = 0$). Here, $s_k(t)$ denotes the signal from the k-th source, and $n_m(t)$ denotes the additive Gaussian white noise at the m-th sensor with variance σ^2 and zero mean. Therefore, the full array of the received signal is expressed as:

$$\mathbf{y}(t) = \mathbf{A}\mathbf{s}(t) + \mathbf{n}(t) \tag{2}$$

where $\mathbf{y}(t) = [y_{-N}(t), \ldots, y_0(t), \ldots, y_N(t)]^T$, $\mathbf{s}(t) = [s_1(t), \ldots, s_K(t)]^T$, $\mathbf{n}(t) = [n_{-N}(t), \ldots, n_0(t), \cdots, n_N(t)]^T$. In addition, the matrix $\boldsymbol{A}$ is the direction matrix defined as $\mathbf{A} = [\mathbf{a}(x_1, y_1), \cdots, \mathbf{a}(x_K, y_K)]$, with the steering vector for the k-th source given by

$$\mathbf{a}(x_k, y_k) = \left[e^{j\frac{2\pi}{\lambda}(d_{-N}^{(k)} - d_0^{(k)})}, \cdots, e^{j\frac{2\pi}{\lambda}(d_N^{(k)} - d_0^{(k)})}\right]^T. \tag{3}$$

A. Multiple Signal Classification - MUSIC 2D

The 2D MUSIC algorithm (Alg. 1) [12], [13] is a high-resolution technique, less complex than many alternatives, for estimating incident signal direction (x, y), taking as input parameters the number of sensors in the array (N), the received signal $\mathbf{Y}$, and the grid - $\mathcal{G}(x, y)$.

The algorithm's computational complexity is dictated by its search grid resolution, which defines the size of a conceptual dictionary of candidate steering vectors to be tested. For a fine 80×80 grid, this dictionary has dimensions of M×(80×80), while a coarse 35×35 grid reduces its size to M×(35×35). This substantial reduction in the search dictionary is the key to lowering the computational load, thus creating a fundamental trade-off between localization accuracy and processing efficiency. The MUSIC 2D steps are detailed next.

Bicubic interpolation, a two-dimensional technique widely used in image processing [14], [15], is employed here to refine the MUSIC pseudo-spectrum. When $P_{\text{coarse}}(x, y)$ is evaluated on a coarse grid to reduce complexity, the true peak may lie between the sampled points. A continuous surface, $P_{\text{interp}}(x', y')$, is estimated, from which the peak location is identified:

$$P_{\text{interp}}(x', y') = \text{Interp}_{\text{bicubic}}\big[P_{\text{coarse}}(x, y)\big],$$
$$(\hat{x}, \hat{y}) = \arg\max_{x', y'} P_{\text{interp}}(x', y'). \tag{4}$$

Algorithm 1: MUSIC 2D Algorithm

Input: $M, K, \mathbf{Y}$, $\mathcal{G}(x, y)$ - Search grid points
Steps:
Compute the sample covariance matrix $\mathbf{R}$
  $\mathbf{R} \leftarrow \frac{1}{L}\mathbf{Y}\mathbf{Y}^H$
Perform eigenvalue decomposition of $\mathbf{R}$
  $(\mathbf{U}, \mathbf{\Lambda}) \leftarrow \text{eig}(\mathbf{R})$
Construct the noise subspace $\mathbf{U}_n$
  $\mathbf{U}_n \leftarrow$ eigenvectors corresponding to the smallest $(M - K)$ eigenvalues
foreach $(x, y) \in \mathcal{G}$ **do**
  Compute the range r_m from each array element m to the point (x, y)
    $d_m \leftarrow \sqrt{(x - x_m)^2 + y^2}$
  Construct the steering vector $\mathbf{a}(x, y)$
    $\mathbf{a}(x, y) \leftarrow [e^{j\frac{2\pi}{\lambda}(d_{-N} - d_0)}, \ldots, e^{j\frac{2\pi}{\lambda}(d_N - d_0)}]^T$
  Evaluate the MUSIC pseudo-spectrum $P_{\text{MUSIC}}(x, y)$
    $P_{\text{MUSIC}}(x, y) \leftarrow \frac{1}{\mathbf{a}^H(x,y)\mathbf{U}_n\mathbf{U}_n^H\mathbf{a}(x,y)}$
end
Output: $P_{\text{MUSIC}}(x, y)$

The interpolated surface is locally modeled as a bicubic polynomial of the form

$$P_{\text{interp}}(x', y') = \sum_{k=0}^{3}\sum_{l=0}^{3} a_{kl}\, x^k y^l, \tag{5}$$

where the coefficients a_{kl} are determined from the values of the 16 nearest samples in a 4×4 neighborhood. This approach retains the high spatial resolution of a dense grid search while incurring only the computational cost of the coarse evaluation.

B. Refinement Procedure

The refinement process applies the standard bicubic interpolation algorithm, whose full details are described in [14], [15]. Given a coarse MUSIC pseudo-spectrum, the procedure for each point on the desired fine grid begins by identifying a corresponding 4×4 neighborhood of samples on the coarse grid. Interpolation weights are then computed based on the point's fractional offsets within its coarse-grid cell, typically using a cubic convolution kernel (e.g., Keys' kernel). The refined value is finally computed as a weighted summation of the 16 neighborhood samples. After populating the fine grid, the estimated source position $(\hat{x}, \hat{y})$ is obtained by identifying the peak value in the interpolated surface.

By combining a coarse MUSIC evaluation with bicubic interpolation, the method achieves accurate localization with significantly reduced computational effort. The initial grid resolution and the refinement level jointly determine the trade-off between accuracy and complexity.

III. Numerical Results

In this section, we present numerical examples. The BS is equipped with a uniform linear array (ULA) of $M = 65$ antennas/sensors. The carrier frequency is set to $f_c = 5$ GHz,

resulting in a wavelength of $\lambda = c/f_c = (3 \times 10^8 \text{ m/s})/(5 \times 10^9 \text{ Hz}) = 0.06$ m. The inter-element spacing is $d = \lambda/4 = 0.015$ m. The total aperture of the array is $D = 2Nd = 64 \times 0.015 \text{ m} = 0.96$ m. To determine the field region, we calculate the Fraunhofer distance, $R_f = \frac{2D^2}{\lambda} = \frac{2\times(0.96 \text{ m})^2}{0.06 \text{ m}} \approx 30$ m. A single source ($K = 1$) is considered, located at the Cartesian coordinate (x, y). Without loss of generality, the search region is limited to $x \in [-6, 6]$ m and $y \in [1, 15]$ m. Since the maximum operational distance in the search region (15 m) is smaller than the Fraunhofer distance ($R_f \approx 30$ m), the scenario is confirmed to be in the **near-field**. The number of snapshots is $L = 100$.

Fig. 1 depicts a fine grid MUSIC pseudo-spectrum computed on a 80×80 search grid with the user placed at $(5, 12)$ m, and SNR = 10 dB. The MUSIC algorithm yields an error of 0.20 m with an execution time of 0.0446 s; in this work, we will use this result as a benchmark.

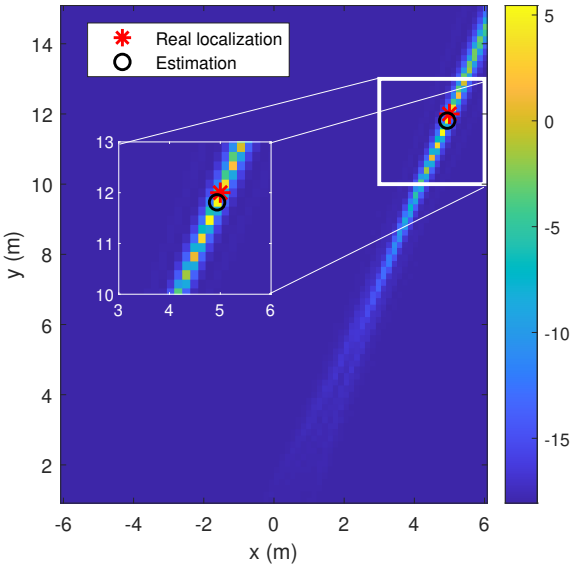

Fig. 1: Fine (grid 80×80) MUSIC pseudo-spectrum with the user located at $K_1(5, 12)$, error = 0.2 m and execution Time = 0.0446 s.

A. Grid Resolution Selection Strategy

We first fix the fine-grid resolution. Preliminary evaluations indicate an 80×80 grid provides sub-meter accuracy. For instance, with a source at $(5, 12)$ m and 10 dB SNR, this grid yields a 0.2 m RMSE (Fig. 1), serving as our benchmark for coarse-to-fine interpolation methods.

To minimize computation while preserving this 0.2 m RMSE, we employ a backward selection strategy considering the RMSE-grid size trade-off. We explore various coarse grid sizes, refine their pseudo-spectra to 80×80 using bicubic interpolation, and then compare the post-interpolation RMSE against our benchmark.

Fig. 2 shows the RMSE and execution time as functions of the coarse grid resolution, while the fine grid remains fixed at 80×80. From this analysis, we observe that a coarse grid of 35×35—refined via bicubic interpolation—achieves an RMSE close to the fine-grid reference (*i.e.*, 0.2 m) while reducing the execution time by a factor of four. The results confirm that

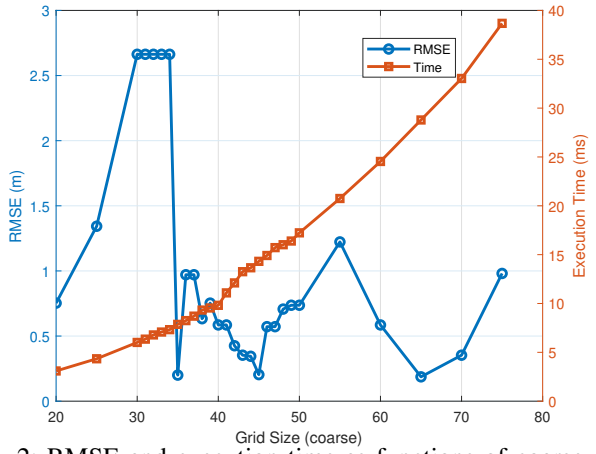

Fig. 2: RMSE and execution time as functions of coarse grid resolution. The pseudo-spectrum is refined to a fixed 80×80 grid using bicubic interpolation.

this configuration provides a near-optimal trade-off between localization accuracy and computational efficiency, making it suitable for real-time ISAC applications.

In summary, the fine grid is fixed based on target RMSE, and the coarse grid is selected based on its ability to preserve that RMSE after interpolation, while minimizing the associated computational cost.

B. Performance Illustration of Bicubic Refinement

To illustrate interpolation's practical effects, Figs. 1, 3, and 4 compare coarse, interpolated, and fine-grid MUSIC pseudo-spectra for a source at $(5, 12)$ m (SNR = 10 dB, L=100 snapshots). The coarse MUSIC (grid 35×35, Fig. 3) yields a 1.19 m localization error. In contrast, fine-grid MUSIC (grid 80×80, Fig. 1) achieves a 0.2 m RMSE, albeit at a higher computational cost. Remarkably, applying bicubic interpolation to the coarse pseudo-spectrum (Fig. 4) matches this 0.2 m accuracy with significantly reduced execution time (0.015 s *vs.* 0.0446 s for fine MUSIC). This confirms bicubic refinement's ability to bridge the resolution gap between coarse and fine grids, enabling real-time operation with negligible performance loss.

C. Performance Comparison over SNR for MUSIC Schemes

To validate the robustness and scalability of the proposed bicubic refinement strategy, 200-trial Monte Carlo simulations were conducted over a wide SNR range, comparing its performance against full-grid (fine) MUSIC, coarse-grid MUSIC, and zoom-in MUSIC [8]. All simulations used previously described parameters, with a 35×35 coarse grid and an 80×80 fine grid. Zoom-in MUSIC parameters, ensuring comparable execution times, are in Table I.

Fig. 5. a) presents the RMSE of the estimated source position versus SNR for four MUSIC-based schemes: (i) Fine MUSIC (exhaustive 80×80 grid), (ii) Coarse MUSIC (35×35 grid), (iii) Coarse MUSIC with bicubic interpolation to an 80×80 mesh, and (iv) Zoom-in MUSIC (refining peak regions with a localized 51×51 high-resolution window). As expected, fine MUSIC consistently achieves the highest accuracy (RMSE below 0.45 m for SNR $\geq$ 10 dB) due to dense sampling. Conversely, coarse MUSIC suffers resolution loss (RMSE $>$ 1 m) from under-sampling. Bicubic interpolation significantly

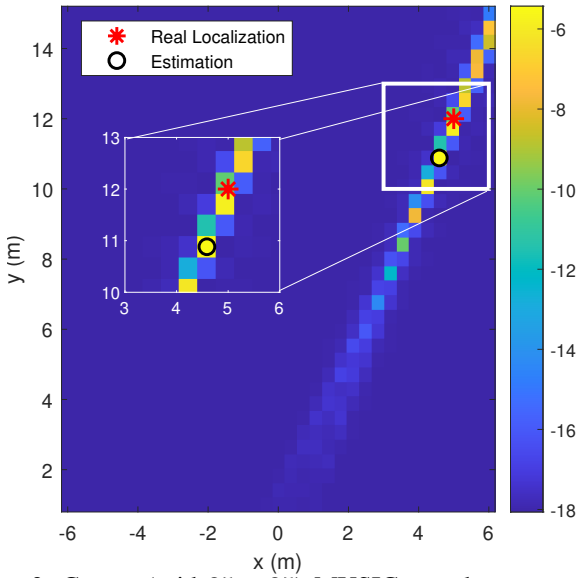

Fig. 3: Coarse (grid 35×35) MUSIC pseudo-spectrum with the user located at $K_1(5, 12)$, error = 1.1911 m and execution time = 0.0134 s.

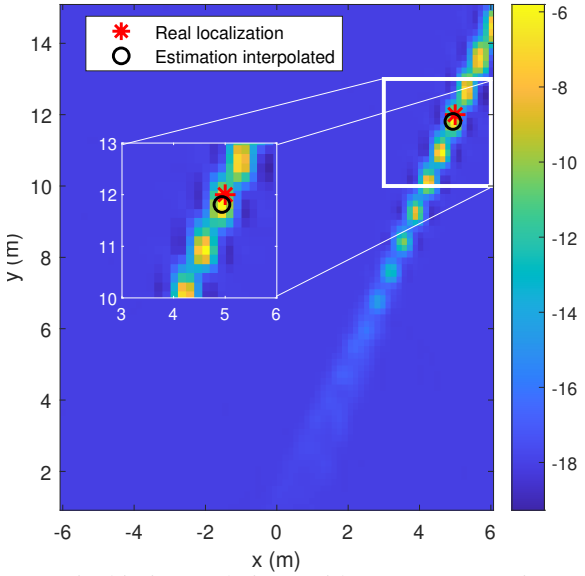

Fig. 4: Bicubic interpolation (grid coarse 35×35 interpolated to 80×80) MUSIC pseudo-spectrum with the user located at $K_1(5, 12)$, error = 0.2 m and execution time = 0.015 s.

enhances performance, refining the coarse pseudo-spectrum to yield RMSE comparable to fine MUSIC for SNRs above 5 dB (sub-meter precision at a fraction of the cost) by reliably approximating sub-grid peaks. Zoom-in MUSIC surpasses coarse MUSIC but is slightly less robust than bicubic interpolation at low SNR (< 0 dB); its accuracy approaches the interpolated method for SNR ≥ 5 dB. In summary, bicubic interpolation offers the best accuracy-complexity trade-off, nearing fine MUSIC's precision without its extensive computation, making it practical for real-time or resource-constrained applications.

Fig. 5. b) displays the average execution time per trial, which is governed by grid size and search strategy rather than SNR, hence the flat curves. Fine MUSIC is most demanding (approx. 0.40 s/trial for its 80×80 grid). Coarse MUSIC has the lowest latency (approx. 0.009 s/trial with its 35×35 grid). The bicubic interpolation adds negligible overhead (0.0005 s) to the coarse estimate, totaling approx. 0.0095 s (a 5–6% increase over coarse MUSIC) yet yielding performance comparable to fine MUSIC. Zoom-in MUSIC, with its localized 51×51 refinement, takes about 0.013 s.

Bicubic interpolation emerges as the most computationally efficient strategy, offering a compelling trade-off between localization precision and cost, particularly for latency-sensitive ISAC scenarios. While fine MUSIC provides the highest accuracy via its exhaustive search, its significant overhead (nearly 40 times slower than bicubic interpolation) makes it less suitable for real-time applications. Bicubic interpolation maintains sub-meter accuracy, especially for SNR ≥ 5 dB, with substantially reduced runtime. Zoom-in MUSIC is a compromise, showing slightly higher noise sensitivity at low SNRs. Therefore, the bicubic refinement method is a practical choice for ISAC systems, bridging high-resolution estimation and real-time feasibility by delivering near-optimal precision with significantly enhanced speed.

TABLE I: Zoom-In MUSIC: Key Parameter Settings

Parameter	Symbol	Value
Coarse grid points	N_c	35
Fine window half-width	W_x, W_y	± 0.5 m
Local fine step	$\Delta x', \Delta y'$	0.02 m
Local grid step	n_ℓ	80
Number of sources	K	1

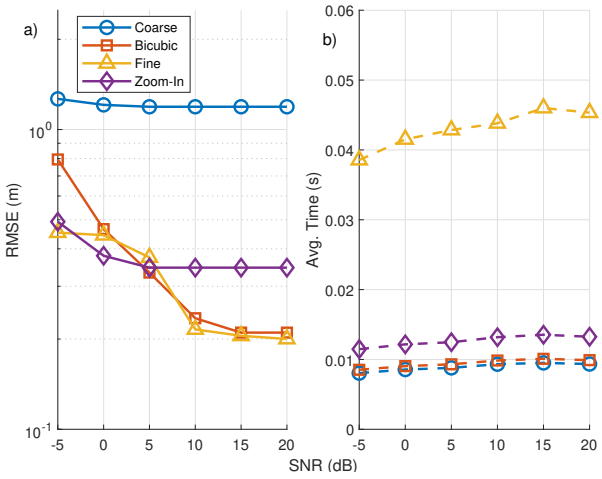

Fig. 5: a) RMSE of real location and estimates and b) Average execution time per trial *vs.* SNR.

D. Computational Complexity Analysis

To provide a quantitative analysis of computational efficiency, we estimate the average number of floating-point operations (FLOPs) required by each MUSIC variant. The calculations consider the dominant operations in pseudo-spectrum evaluation, including steering vector generation, projection onto the noise subspace, and peak search.

Table II summarizes the average FLOP count per trial for coarse MUSIC, fine MUSIC, zoom-in MUSIC, and the proposed bicubic interpolation method. As expected, the fine MUSIC requires the highest number of operations due to its exhaustive search over an 80×80 grid. Coarse MUSIC has

TABLE II: Performance and Complexity Summary of 10 dB MUSIC Variants

Method	Grid	RMSE (m)	Time (s)	FLOPs
Coarse MUSIC	35×35	1.19	0.0090	4.1×10^6
Bicubic Interp.	$35 \rightarrow 80$	0.21	0.0095	4.3×10^6
Zoom-In MUSIC	$35/51$	0.35	0.0130	6.5×10^6
Fine MUSIC	80×80	0.20	0.0446	9.6×10^6

the least complexity, followed closely by the bicubic-refined version, which introduces negligible overhead thanks to the efficient interpolation process. The zoom-in strategy exhibits intermediate complexity, balancing global and local search.

These results validate the proposed method as a computationally efficient alternative to full-grid MUSIC, achieving near-optimal accuracy at a fraction of the cost. This characteristic is particularly relevant for real-time systems with strict latency and resource constraints, such as ISAC applications in 6G.

In MUSIC-based localization, the computational burden comprises covariance formation[16] $\mathcal{O}(2M^2N_t)$, eigenvalue decomposition $\mathcal{O}\big(\frac{9}{2}M^3\big)$, and pseudo-spectrum search. In the full-grid (fine) MUSIC, evaluating $n_f \times n_f$ points adds $\mathcal{O}(M^2 n_f^2)$ FLOPs, yielding a total of

$$\mathcal{O}\big(2M^2N_t + \tfrac{9}{2}M^3 + M^2 n_f^2\big).$$

In the coarse MUSIC, reducing to an $n_c \times n_c$ grid lowers this to

$$\mathcal{O}\big(2M^2N_t + \tfrac{9}{2}M^3 + M^2 n_c^2\big).$$

When coarse MUSIC is followed by bicubic interpolation on an $n_i \times n_i$ fine mesh, an extra $\mathcal{O}(n_i^2)$ term appears, for

$$\mathcal{O}\big(2M^2N_t + \tfrac{9}{2}M^3 + M^2 n_c^2 + n_i^2\big).$$

In Zoom-In refinement, each of the K local windows of size $n_\ell \times n_\ell$ incurs $\mathcal{O}(2M^2 n_\ell^2)$ FLOPs, totaling

$$\mathcal{O}\big(K\, M^2 n_\ell^2\big).$$

These results (summarized in Table II at 10 dB) confirm that coarse-grid MUSIC with bicubic interpolation adds negligible overhead to the pure coarse search, while zoom-in MUSIC incurs a higher but still sub-fine-grid cost.

In summary, the computational complexity analysis confirms that the proposed bicubic interpolation scheme provides an excellent trade-off: it preserves near-optimal localization accuracy with minimal added cost compared to pure coarse MUSIC. Fine MUSIC, although accurate, incurs a prohibitive complexity for real-time operation. Zoom-in MUSIC strikes a middle ground but still demands substantially more processing than the interpolated variant. These findings further support the practical viability of the bicubic method in ISAC scenarios, especially when low-latency processing and hardware constraints are critical design factors.

IV. Conclusion

This paper introduced a bicubic-interpolation-enhanced MUSIC framework for ISAC systems. The pseudo-spectrum, first evaluated on a coarse Cartesian grid, is then interpolated to fine resolution using standard bicubic kernels. By transforming the coarse Cartesian grid into polar coordinates for steering-vector computation, the method seamlessly integrates interpolation without additional coordinate-domain complications. Extensive Monte Carlo simulations demonstrate that this approach achieves near-fine-grid localization accuracy (sub-meter RMSE for SNR ≥ 5 dB) while reducing computational time by up to 75 % compared to exhaustive fine-grid MUSIC.

Future work will address multi-target scenarios and large-scale antenna arrays, compare the proposed bicubic-enhanced MUSIC against other promising complexity-reduction techniques, investigate adaptive grid-selection heuristics to further reduce interpolation overhead, and validate performance under realistic channel models and hardware constraints.

The simplicity and effectiveness of bicubic refinement make it a compelling candidate for real-time ISAC deployments.

References

[1] F. Liu, W. Yuan, C. Masouros, J. Yuan, and L. Hanzo, "Integrated sensing and communications: Towards dual-functional wireless networks for 6g and beyond," *IEEE Journal on Selected Areas in Communications*, vol. 40, no. 6, pp. 1728–1767, 2022.

[2] H. Wymeersch, J. He, B. Denis, A. Clemente, and M. Juntti, "Radio localization and mapping with reconfigurable intelligent surfaces," *IEEE Communications Magazine*, vol. 58, no. 6, pp. 61–67, 2020.

[3] X. Cao, A. Chen, H. Yin, and L. Chen, "A low-complexity near-field localization method based on electric field model," *IEEE Communications Letters*, vol. 28, pp. 288–292, Feb. 2024.

[4] Y. Gao, M. Wu, C. Hao, and Y. Wu, "Near-field source localization using the spice method for limited snapshots," in *2024 7th International Conference on Information Communication and Signal Processing (ICICSP)*, pp. 1–5, 2024.

[5] S. Lv, J. Pan, H. Pan, Y. Ning, and Y. Wang, "Near-field coherent source localization for two closely located sources," in *2024 IEEE 24th International Conference on Communication Technology (ICCT)*, pp. 768–772, 2024.

[6] M. Cao, H. Zhang, B. Di, and H. Zhang, "Unified near-field and far-field localization with holographic mimo," in *2024 IEEE Wireless Communications and Networking Conference (WCNC)*, pp. 1–6, 2024.

[7] Y. Pan and G. Q. Luo, "Efficient direction-of-arrival estimation via annihilating-based denoising with coprime array," *Signal Processing*, vol. 184, p. 108061, 2021.

[8] X. Zhang, W. Chen, W. Zheng, Z. Xia, and Y. Wang, "Localization of near-field sources: A reduced-dimension music algorithm," *IEEE Communications Letters*, vol. 22, no. 7, pp. 1422–1425, 2018.

[9] L. Zhang, Y. Sun, X. Xie, Z. Tian, Y. Xing, and F. Chen, "Image restoration based on partial least squares regression and wavelet bi-cubic ratio interpolation," in *2013 6th International Congress on Image and Signal Processing (CISP)*, vol. 01, pp. 379–383, 2013.

[10] X. Liu, Y. Meng, Z. Zhang, J. Li, Y. Gong, Y. Lei, C. Yang, and L. Geng, "Efficient bicubic interpolation architecture for rgb image data stream," in *2023 6th International Conference on Electronics Technology (ICET)*, pp. 1356–1361, 2023.

[11] R. Boyer and J. Picheral, "Second-order near-field localization with automatic paring operation," in *2008 IEEE International Conference on Acoustics, Speech and Signal Processing*, pp. 2569–2572, 2008.

[12] A. Swindlehurst and T. Kailath, "A performance analysis of subspace-based methods in the presence of model errors. i. the music algorithm," *IEEE Transactions on Signal Processing*, vol. 40, no. 7, pp. 1758–1774, 1992.

[13] R. Schmidt, "Multiple emitter location and signal parameter estimation," *IEEE Transactions on Antennas and Propagation*, vol. 34, no. 3, pp. 276–280, 1986.

[14] R. G. Keys, "Cubic convolution interpolation for digital image processing," *IEEE Transactions on Acoustics, Speech, and Signal Processing*, vol. 29, no. 6, pp. 1153–1160, 1981.

[15] R. C. Gonzalez and R. E. Woods, *Digital Image Processing*. Pearson, 3rd ed., 2008.

[16] G. H. Golub and C. F. V. Loan, *Matrix Computations*. Baltimore, MD: Johns Hopkins University Press, 4th ed., 2013.